Thermodynamic Theory of Network-Forming Polymer Solutions. 2. Equilibrium Gelation by Conterminous Cross-Linking

Fumihiko Tanaka

Department of Physics, Faculty of General Education, Tokyo University of Agriculture and Technology, Fuchu-shi, Tokyo, 183 Japan

Received December 5, 1989; Revised Manuscript Received February 15, 1990

ABSTRACT: This paper studies equilibrium phase behavior of the polymer solution in which long polymer chains are conterminously cross-linked by short chains or solvent molecules. It is shown that the sol–gel transition line exhibits a maximum at certain polymer concentration on the temperature–concentration plane. We focus our attention on the characteristic features caused by the interference between gelation and phase separation. Comparison of the theoretical results with the existing DSC data on the gel melting line for atactic polystyrene in carbon disulfide is detailed.

1. Introduction

Since the discovery[1] that certain chemically inactive atactic polystyrene (at-PS) solutions can exhibit gelation, there has been a growing interest[2–6] in the phenomena of physical gelation. Recent experimental studies have furnished strong evidence that the at-PS gelation is thermally reversible and can be a universal phenomenon that takes place in a wide variety of solvents. The current understanding of the experimental observations is based on the cooccurrence of the sol–gel transition and two-phase separation on the temperature–concentration plane. In our recent paper,[7,8] we pointed out the possibility of the appearance of a tricritical point or a three-phase equilibrium temperature as a result of the interference between the two inherently different phase transitions, if the solute–solvent combination and their molecular weights are judiciously chosen. Among many unsolved questions on the physical gelation, one of the most important problems is concerned with the molecular mechanism of cross-linking. Although the origin of associative interchain interaction has not been clarified, the binding energy connecting a pair of the polymer segments is expected to be on the order of thermal energy. This enables the system to reach thermal equilibrium. The main purpose of the present paper is to examine the molecular origin of the association.

Figure 1 shows the experimental data on the gel melting points of the at-PS/CS_2 system on the temperature–concentration plane obtained by two different methods. The upper group consists of the melting points found by the differential scan calorimetry (DSC)[9] in heating processes for four different molecular weights of at-PS ranging from 6×10^3 to 5.6×10^6. The lower group consists of those found by rheological measurement such as the tilting flow method and the ball-drop method for three different molecular weights ranging from 9.06×10^4 to 2.53×10^5. Polymer concentration is reduced to the volume fraction by using the density of PS (1.05 g/cm^3) and CS_2 (0.256 g/cm^3), while the temperature is measured in the dimensionless deviation $\tau \equiv 1 - \Theta/T$ from the Θ temperature (Θ = 200 K for at-PS/CS_2). In our previous paper[7,8] we analyzed the rheological data (lower group) under the assumption that certain special stereoregular sequences along a chain can directly form interchain bonds. We found that the transition line is a monotonically increasing function of the polymer concentration as the experiment suggests. Recent DSC data[9] (upper group), however, exhibit a maximum at a certain concentration.

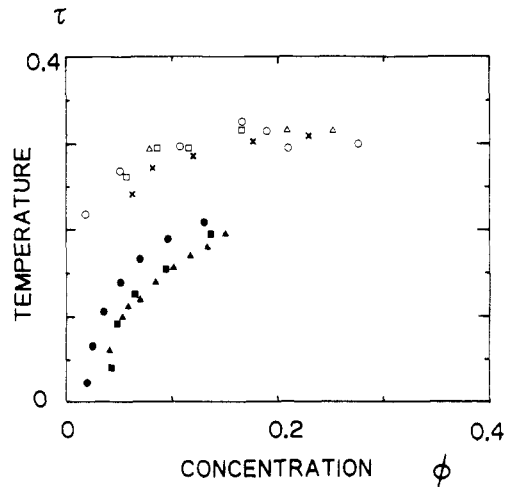

Figure 1. Observed gel melting points for at-PS/CS_2 shown on the temperature–concentration plane. Data measured by DSC: (×) $M_w = 6 \times 10^8$; (○) $M_w = 1.8 \times 10^5$; (△) $M_w = 1.7 \times 10^6$; (□) $M_w = 5.6 \times 10^6$. Data measured by test-tube tilting method and ball-drop method: (■) $M_w = 9.7 \times 10^4$; (●) $M_w = 2.65 \times 10^5$; (▲) $M_w = 2.79 \times 10^5$.

Together with another observation of a maximum in melting enthalpy, the authors of ref 9 concluded that interchain bridging is due to complex formation involving the solvent molecules. Although the discrepancy in the experimental data is not clear at present, existence of a maximum in the sol–gel line is worth our attention. We aim at examining the phase behavior of physical gels formed by solvent complexation in this paper.

Consider a mixture consisting of polymer chains A and cross-linkers B. A cross-linking molecule B is allowed to be either a shorter polymer chain or a small molecule of the size of the monomeric unit. We assume that a cross-linker has reactive groups at both its ends and can form a bridge between A chains by making conterminous bonds with certain reactive groups on the A chains (see Figure 2). In thermal equilibrium, clusters having a wide range of aggregation numbers are reversibly formed. The cross-linkers in the system fall into one of the three categories: free (as in Figure 2a) bound (as in Figure 2b), and dangling (as in Figure 2c). When solvent molecules work as a cross-linker, a bound solvent, together with the two A-chain segments at both its ends, should be regarded as a solvent complex. Authors of ref 9 suggested that, by examining a space-filling model of at-PS, the cavity formed by a syndiotactic triad can capture a CS_2 molecule.

0024-9297/90/2223-3790$02.50/0

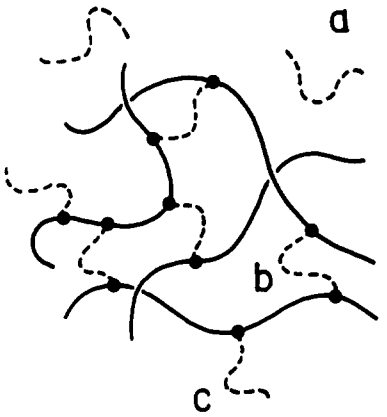

Figure 2. Schematical picture of a cluster formed by conterminous cross-linking. Solid lines show long A chains and broken lines short-chain cross-linkers. A cross-linker is either free (a), bound (b), or dangling (c).

In section 2, we apply our general theory[10] of network-forming polymer solutions to this specific model. Thermodynamic properties are solved in sections 3 and 4. We find the cluster distribution function, sol-gel transition line, and stability limit (spinodals) of the system. Effect of the dangling cross-linkers is discussed in section 3. Detailed comparison of the theoretical results with the experimental data is made in section 5.

2. Thermodynamic Model

We must first specify the quantities on which our system will depend. These will be as follows: V, the total volume of the system; a, the size of a statistical unit constituting the polymer chains; n_A, the number of the statistical units on an A chain; n_B, the number of the statistical units on a B chain (we set $n_B = 1$ for low molecular weight cross-linkers); $\Omega \equiv V/a^3$, the number of the lattice cells in the system. We have assumed, for simplicity, that the size of a statistical unit is the same for A chains and B chains. Let N_A be the number of A chains in the system and N_B be the number of B chains. The volume fraction of each species is then given by $\phi_A = n_A N_A/\Omega$ and $\phi_B = n_B N_B/\Omega$. Because the relation $\phi_A + \phi_B = 1$ holds under incompressible conditions, we write $\phi_A = \phi$ and $\phi_B = 1 - \phi$ in the following.

In thermal equilibrium the system contains clusters formed by interchain bridges, and a macroscopic network might be included among them under certain conditions. As in the preceding paper[10] (hereafter refered to as 1), let (l,m) stand for a type of a cluster that is made up of l A chains and m cross-linkers. The volume fraction, $\phi_{l,m}$ (and hence the number $\nu_{l,m} = \phi_{l,m}/(n_A l + n_B m)$ in a unit volume), of the clusters of the type (l,m) can be determined by the multiple equilibria conditions $l\mu_A + m\mu_B = \mu_{l,m}$ imposed on their chemical potentials. In our paper 1, we constructed the free energy of the network-forming polymer solutions from a general point of view. It is given by the sum of the reaction term and the mixing term. Chemical potentials are derived from the free energy. Following the general procedure shown in 1, we are led to the result

$$\phi_{l,m} = K_{l,m}(\phi_{1,0})^l(\phi_{0,1})^m \tag{2.1}$$

after imposing multiple equilibria, where $\phi_{1,0}$ and $\phi_{0,1}$ are the volume fraction of the isolated A chains (A unimers) and the isolated B chains (B unimers), respectively. Association constants $K_{l,m}$ are expressed as

$$K_{l,m} = \exp(l + m - 1 - \Delta_{l,m}) \tag{2.2}$$

in terms of the free energy change, $\Delta_{l,m}$, for the cluster formation:

$$\Delta_{l,m} = \beta(\mu_{l,m}^\circ - l\mu_A^\circ - m\mu_B^\circ) \tag{2.3}$$

To find the specific form of $K_{l,m}$, we now proceed to the study of the internal free energy, $\mu_{l,m}^\circ$, for a single isolated (l,m) cluster. This is the free energy required to form a cluster with l A chains and m B chains. The canonical partition function of the cluster, whose logarithm is $\mu_{l,m}^\circ$, can be written as

$$Z_{l,m} = \frac{w_{l,m}}{l!m!}p^{m+l-1}(1-p)^{fl-2l+2} \tag{2.4}$$

where p is the equilibrium degree of association, and $w_{l,m}$ is the number of combinations in which l A chains and m B chains may form an (l,m) cluster in the form of the Cayley tree. Intracluster cross-linking is excluded so that no internal loops can appear.[11] Under such conditions, we have $l-1$ bound B chains and $m-l+1$ dangling B chains. The number of bonds in the cluster is $2(l-1) + (m-l+1) = m+l-1$. The number of reactive groups on the A chain that remain unbonded is $fl - (m+l-1) = fl - l - m + 1$, while the number of unreacted B ends is $m - l + 1$. Hence, we have the total number of $fl - 2l + 2$ of unbonded reactive groups.

The number of combinations, $w_{l,m}$, was found by Stockmayer[11] in his pioneering work on branched polymers generated in a polyesterification reaction. It is given by

$$w_{l,m} = \frac{f^l 2^m (fl-l)!m!}{(fl-l-m+1)!(m-l+1)!} \tag{2.5}$$

in our present notation. Definition of $\Delta_{l,m}$ leads to

$$e^{-\Delta_{l,m}} = Z_{l,m}/(Z_{1,0})^l(Z_{0,1})^m = \omega_{l,m}f^l 2^m (e^{-\beta\Delta f_0})^{l+m-1} \tag{2.6}$$

where Δf_0 is the free energy change of a single-bond formation, and

$$\omega_{l,m} = \frac{(fl-l)!}{l!(fl-l-m+1)!(m-l+1)!} \tag{2.7}$$

In eq 2.6, p has been eliminated in favor of Δf_0 by using the equilibrium condition $p/(1-p)^2 = \exp(-\beta\Delta f_0)$ for a bond formation.

We next introduce a shift factor, $\lambda(T)$, defined by $\lambda \equiv \exp(1 - \beta\Delta f_0)$. This factor is a function of the temperature and, as we will see in the following, concentration variables always appear in combination with λ. By using λ, the association constants can be expressed as

$$\lambda K_{l,m} = \omega_{l,m}(f\lambda)^l(2\lambda)^m \tag{2.8}$$

Substitution of this form into eq 2.1 yields

$$\lambda\phi^S(x,y) = \sum_{l,m}\omega_{l,m}x^l y^m \tag{2.9}$$

for the volume fraction ϕ^S of the sol part in the system, and

$$\lambda\nu^S(x,y) = \sum_{l,m}\frac{\omega_{l,m}}{n_A l + n_B m}x^l y^m \tag{2.10}$$

for the number concentration ν^S of finite clusters, where $x \equiv f\lambda\phi_{1,0}$ and $y \equiv 2\lambda\phi_{0,1}$ are the scaled unimer concentrations for each species. In the pregel regime where no macroscopic network exists, we have $\phi^S(x,y) = 1$. On the other hand, in the postgel regime where a macronetwork appears, we have $\phi^S(x,y) < 1$, since the infinite sum in eq 2.9 does not accommodate the contribution from the macronetwork. In Appendix A, we will show detailed calculation to find the functional forms of the double

infinite series on the right-hand side of eqs 2.9 and 2.10. The final results are

$$\lambda\phi^{S}(x,y) = y/2 + [(1+y)^2/y]\, G_0(z) \tag{2.11}$$

and

$$\lambda\nu^{S}(x,y) = \frac{1}{n}\left\{\frac{y}{2b} + \int_0^{\infty}\frac{(1-ye^{-bt})^2}{ye^{-bt}}\, G_0(z(t))\, dt\right\} \tag{2.12}$$

where

$$z \equiv xy(1+y)^{f-2} \tag{2.13}$$

and $n \equiv n_A + n_B$, $a \equiv n_A/n$, $b \equiv n_B/n$, and $z(t) \equiv xye^{-t}(1 + ye^{-bt})^{f-2}$. The functions $G_k(z)$ for integer k are defined by

$$G_k(z) \equiv \sum_{m=1}^{\infty} m^k \omega_m z^m \tag{2.14}$$

as in 1 by using the combinatorial factor $\omega_m = (fm-m)!/m!(fm-2m+2)!$. The parameter z consists of a special combination of the unimer concentrations, but it reduces to a simple product $z = xy$ if the effect of the dangling cross-linkers is neglected. All these results are limited to the region on the (x,y) plane inside which the double power series converges.

3. Small Cross-Linkers

To study solvent complexation, we confine ourselves in the following to the case of low molecular weight cross-linkers for which $a \sim 1$ and $b \ll 1$ holds. When the limit $b \to 0$ is taken, eq 2.12 reduces to the simplified form

$$\lambda\nu^{S}(x,y) = \frac{1}{n}\left\{\frac{y}{2b} + \frac{(1+y)^2}{y}\, G_{-1}(z)\right\} \tag{3.1}$$

where z is given by eq 2.13. Hereafter we follow the general recipe developed in 1 for the study of the thermodynamic properties. In the pregel regime, the double power series converges, so that we have $\phi_A^{S} = \phi$ and $\phi_B^{S} = 1-\phi$. The coupled equations $n_A x(\partial\nu^{S}/\partial x) = \phi$ and $n_B y(\partial\nu^{S}/\partial y) = 1-\phi$ then lead to

$$x = \frac{\lambda\phi z}{(1+y)^f\, G_0(z)} \tag{3.2}$$

and

$$y = 2\lambda(1-\phi) \tag{3.3}$$

The remark that $\phi_{0,1} = 1-\phi$ always holds, so that the volume fraction of the bound cross-linkers is negligibly small in our approximation. From the definition (eq 2.13), we find an equation for z

$$f\, G_0(z) = \frac{\Lambda\phi(1-\phi)}{[1+2\lambda(1-\phi)]^2} \tag{3.4}$$

where $\Lambda \equiv 2f\lambda^2$ is a temperature-dependent parameter. Solving this equation for z yields the functional dependence, $z(\phi)$, on the total composition ϕ.

To study the stability of the system, let us now calculate the κ function[10] for each species. With the help of eq 3.2 we find

$$\kappa_A(\phi) \equiv \phi\, d(\ln x)/d\phi = \frac{\phi}{1+2\lambda(1-\phi)} \times \left\{\frac{1-2(f-3)\lambda(1-\phi)}{1-\phi} + \frac{\Lambda[1-2\phi+2\lambda(1-\phi)]}{fG_1(z)[1+2\lambda(1-\phi)]^2}\right\} \tag{3.5}$$

after lengthy calculation. The identity $z\, G_0'(z) = G_1(z)$ has been used to get eq 3.5. The parameter z must be substituted by its functional form $z(\phi)$ in this equation. Elimination of z in favor of ϕ is explicitly shown in Appendix B.

In a similar way we find

$$\kappa_B(\phi) \equiv -(1-\phi)\, d(\ln y)/d\phi = 1 \tag{3.6}$$

for the cross-linker within our approximation. Having obtained the κ functions, we are prepared to study the spinodal curves that should satisfy

$$\frac{\kappa_A(\phi)}{n_A\phi} + \frac{\kappa_B(\phi)}{n_B(1-\phi)} - 2\chi = 0 \tag{3.7}$$

where χ is Flory's χ-parameter of A/B interaction (see ref 1 for details).

4. Sol–Gel Transition

In our paper 1, we showed that the sol–gel transition takes place when a point (x,y) on the (x,y) plane is located on the boundary line outside of which the infinite series (eq 2.9) diverges. In our present case the boundary is given by the radius of convergence $z^* = (f-2)^{f-2}/(f-1)^{f-1}$ for the function $G_0(z)$. The transition line on the (x,y) plane is therefore given by the condition

$$x^*y^*(1+y^*)^{f-2} = z^*\ (=\text{constant}) \tag{4.1}$$

Because we have $fG_0(z^*) = 1/2(f-2)$, the line is mapped onto the real temperature–concentration plane as

$$\frac{2f\lambda^2\phi(1-\phi)}{[1+2\lambda(1-\phi)]^2} = \frac{1}{2(f-2)} \tag{4.2}$$

This is the sol–gel transition line, which we will compare with the experimental observations. Complicate ϕ dependence suggests that the Ferry–Eldridge procedure to find the enthalpy of gelation is inadequate for solvent complexation. If we neglect the effect of the dangling cross-linkers, the transition line is obtained as

$$\phi(1-\phi) = \frac{1}{4f(f-2)\lambda(T)^2} \tag{4.3}$$

The minimum of $\lambda(T)$, and hence the maximum of the transition temperature, as a function of the concentration is therefore reached at the concentration $\phi_{max} = 0.5$. We will see in the numerical calculation that consideration of the dangling cross-linkers does not alter the result to any great extent.

In the postgel regime, unimer concentration y^* of the cross-linker must satisfy the condition $n_B y^*(\partial\nu^{S}/\partial y)_{x^*,y^*} = \phi_B^{S}$ (=$1-\phi$ in our approximation), giving

$$y^*(\phi) = 2\lambda(1-\phi) \tag{4.4}$$

just as in the pregel regime. The unimer concentration x^* is found to be

$$x^*(\phi) = \frac{z^*}{2\lambda(1-\phi)[1+2\lambda(1-\phi)]^{f-2}} \tag{4.5}$$

from eq 4.1.

Let us now find the volume fraction of the gel network. The volume fraction ϕ_i^{S} of each species in the sol part is given by

$$\phi_A^{S} = n_A x^*\left(\frac{\partial\nu^{S}}{\partial x}\right)_{x^*,y^*} = \frac{[1+2\lambda(1-\phi)]^2}{2\Lambda(f-2)(1-\phi)} \tag{4.6}$$

and

$$\phi_B{}^S = n_B y^* \left(\frac{\partial \nu^S}{\partial y}\right)_{x^*,y^*} = 1 - \phi \tag{4.7}$$

Hence, we have $\phi_B{}^G = 0$ and

$$\phi_A{}^G = \phi - \frac{[1 + 2\lambda(1-\phi)]^2}{2\lambda(f-2)(1-\phi)} \tag{4.8}$$

for the gel volume fraction. The κ function in this post-gel regime can be found by

$$\kappa_A{}^*(\phi) = \phi \frac{d}{d\phi}\left(1 + \phi_A{}^G \frac{d}{d\phi}\right) \ln x^*(\phi) \tag{4.9}$$

for A chains and $\kappa_B{}^*(\phi) = 1$ for the cross-linkers.

5. Results of Numerical Calculations and Comparison with the Experiments

To compare the theoretical prediction with the DSC measurement[9] on the at-PS/CS_2 system, let us specify the numerical parameters on which the actual system depends. We first split the free energy Δf_0 of a bond formation into the energy and entropy terms

$$\beta \Delta f_0 = \beta \Delta \epsilon - \Delta s / k_B \tag{5.1}$$

where $\Delta\epsilon$ (<0) is the energy change and Δs the entropy change required for a bond formation. We then have

$$\lambda = \lambda_0 \exp(-\beta \Delta \epsilon) \tag{5.2}$$

for the temperature shift factor, where $\lambda_0 \equiv \exp(1 + \Delta s/k_B)$ is a temperature-independent parameter. Since a certain degree of freedom in molecular orientation is lost when a bond forms, Δs is normally negative and hence λ_0 is expected to be a small numerical constant.

We measure the temperature by the dimensionless deviation $\tau \equiv 1 - \Theta/T$ from the Θ temperature. Near around Θ, the Flory interaction parameter is known[12] to obey in most cases the formula

$$\chi = 1/2 - \psi_1 \tau \tag{5.3}$$

Here an amplitude ψ_1 takes a numerical value of order unity, the precise value of which is dependent on the solute–solvent combination. In terms of the reduced temperature, $\beta\Delta\epsilon$ can be written as

$$\beta \Delta \epsilon = -r(1 - \tau) \tag{5.4}$$

where $r \equiv -\Delta\epsilon/k_B\Theta$ (>0) is the dimensionless bonding energy measured relative to the thermal energy.

We have six parameters specifying chemical constituents of the system: n_A, DP of an A chain; n_B, DP of a cross-linker; f, functionality of an A chain; λ_0, entropy parameter; r, bonding energy/thermal energy; ψ_1, contact interaction between A and B monomers.

In the following analysis we fix $\psi_1 = 1.0$. Since the molecular weight of at-PS in the DSC experiment is typically on the order of 10^6, we choose $n_A = 500$ and $n_B = 1$. This corresponds to 2×10^3 for the molecular weight of a statistical unit of a PS chain. Because the number of syndiotactic triads on a chain is expected to be $(1/2)^3 \cdot n_A$ if the chain has random tacticity, we also fix $f = 50$. Clearly these values are rather arbitrary and were chosen so as to make the final calculation as simple as possible, while maintaining physical reasonableness. The effect of the bonding free energy is examined by changing r and λ_0.

Figure 3 shows the comparison of the predicted sol–gel transition line with the experimental data. Theoretical curves are plotted against the polymer volume fraction.

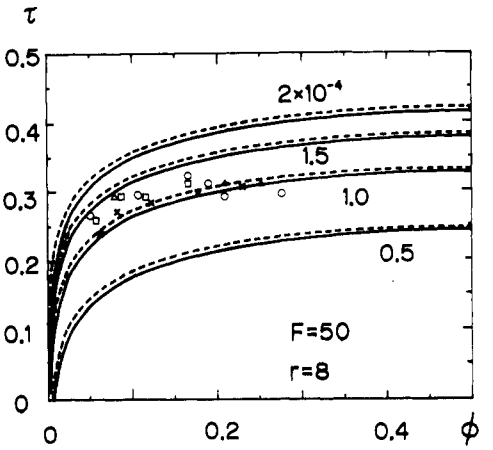

Figure 3. Calculated sol–gel transition lines compared with the experimental data. The entropy parameter is changed from curve to curve. Solid liies are results obtained by the full equation (eq 4.2) and broken lines by approximation (eq 4.3) in which dangling cross-linkers are neglected.

Thick solid lines show the calculation based on eq 4.2, while the broken lines are obtained within the approximation (eq 4.3) in which the dangling cross-linkers are neglected. For low molecular weight cross-linkers the two results exhibit only minor quantitative difference. The concentration is measured in the volume fraction (instead of the weight fraction as was done in the experiment). This is because the gelation is related to the change in spatial connectivity for which an occupied volume of the substance is more important than weight. The molecular weight dependence of the theoretical curve is virtually absent once the f value is fixed, but, as stated above, f should be regarded as proportional to the molecular weight. When f is increased, the transition line shifts to a higher temperature and low-concentration region. The theoretical curves are fit by adjusting the entropy parameter, λ_0. Figures alongside the curves stand for λ_0. Small values of λ_0 suggest that very large entropy loss is associated with solvent comlexation. The concentration at which the transition curve reaches maximum is lower in the experimental data than in the theoretical calculation. Another conclusion we can draw from the calculation is that a large value of r ($r = 8$) is required to fit the data in the dilute region. The experimental data even indicate a finite transition temperature when extrapolated into the vanishing polymer concentration. Since this is clearly unphysical, there remains some doubt on the DSC measurement in the extremely dilute region.

Figure 4 shows the transition line (broken line) together with the spinodal curve (solid line). The parameters are fixed as in Figure 3. A very high value of r pushes the lower concentration branch of the spinodal to the extremely dilute region, which cannot be seen clearly in this scale of the concentration. For comparison, we show in Figure 5 the result for a lower value of r ($r = 6$). We can see the lower branch in this figure, but the transition line appears at so lower temperatures that it cannot be fit to the experimental data. The spinodal line jumps at the intersection with the gelation line, thus indicating discontinuity in the osmotic compressibility. As discussed in our previous paper,[10] the intersection of the gelation line and the spinodal (or more precisely the binodal) is a tricritical point.

Figure 6 shows the decomposition of the total polymer concentration into the gel fraction and the sol fraction. In this figure ϕ^S stands for the sol volume fraction of A chains, ϕ^G for the gel volume fraction, $\phi_{1,0}$ for the volume fraction

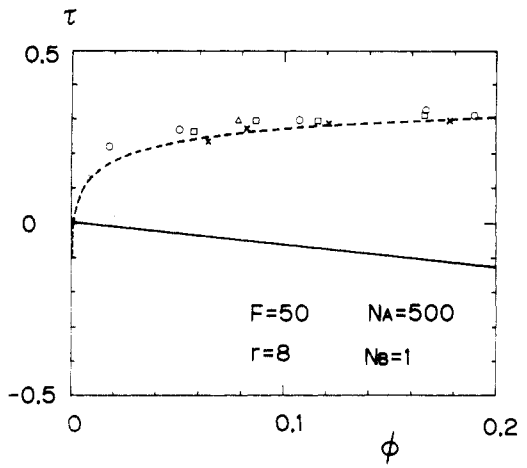

Figure 4. Theoretical sol–gel line (broken line) and spinodal line (solid line) on the temperature–concentration plane. Below the spinodal the system is thermally unstable.

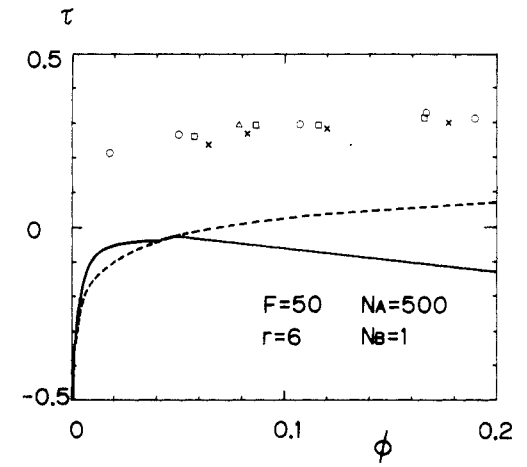

Figure 5. Same as in Figure 3 for a smaller value of r. A tricritical point appears at the intersection of the gelation line and the spinodal line, where there is a discontinuity in the osmotic compressibility.

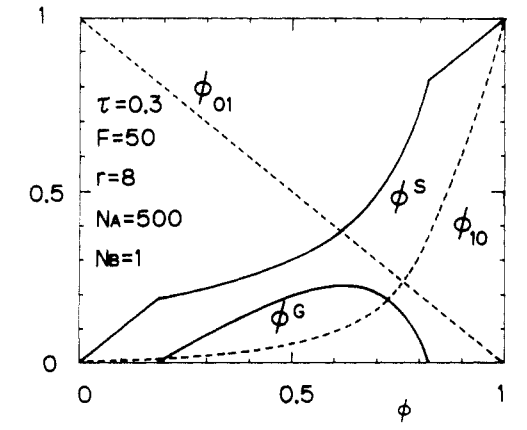

Figure 6. Sol volume fraction, ϕ^S, gel volume fraction, ϕ^G, volume fraction of isolated A chains, $\phi_{1,0}$, and of the isolated cross-linkers, $\phi_{0,1}$, shown as a function of the total polymer concentration. Gel appears in the intermediate concentration range. The temperature is fixed at $\tau = 0.3$.

of the isolated polymer chains, and $\phi_{0,1}$ for the volume fraction of the isolated cross-linkers. Because the temperature is fixed at $\tau = 0.3$, the gel exists in an intermediate concentration range as can be seen from Figure 3. The relation $\phi_{0,1} = 1 - \phi$ always holds in our approximation for low molecular weight cross-linkers.

6. Conclusions and Discussion

From the theoretical results obtained in this paper, the following conclusions are evident:

(1) If segment association between at-PS chains is caused by solvent complexation, there should be a maximum temperature in the sol–gel transition line. This must be around the concentration $\phi = 0.5$ in the *volume fraction*.

(2) For sufficiently low temperatures the connectivity becomes large enough for gel formation in an *intermediate concentration range*. The system exhibits a reentrant sol phase at sufficiently high polymer concentration.

(3) Observed molecular weight dependence of the transition point indicates that the functionality f of a randomly atactic PS chain is proportional to the chain length and hence that some stereoregular sequences on a chain are responsible for solvent complex formation.

(4) Large entropy is lost due to the strong orientational constraint when a bond is formed between a pair of at-PS polymer segments in the help of a solvent molecule.

(5) The binding energy of a bond is several times larger than the thermal energy.

Any revision in method for measuring the sol–gel transition will provide a more precise test of the above conclusions deduced from our molecular theory.

Clearly the model we proposed is rather crude in the sense that the entire picture is based on the molecular field approximation. It is chosen so as to make the final calculation as clear as possible. Any of the revisions for achieving a better fit to the experimental data, however, would greatly complicate application to a real system.

Calculations performed in this paper encourage the expectation that our general theory of network-forming polymer solutions may be broadly applicable to the enormous systems of practical interest.

Appendix A

In this appendix we sum up the double series in eqs 2.9 and 2.10. We first isolate the $(l,m) = (0,1)$ term and then introduce q defined by $q \equiv m - l + 1$. After some rearrangement the right-hand side of eq 2.9 can be transformed into

$$\sum_{l,m}\omega_{l,m}x^l y^m = \frac{y}{2} + \sum_{l=1}^{\infty}\frac{(fl-l)!}{l!(fl-2l+2)!}\times \left\{\sum_{q=0}^{fl-2l+2}\frac{(fl-2l+2)!}{(fl-2l-q+2)!q!}y^q\right\}x^l y^{l-1}$$

$$= \frac{y}{2} + \frac{(1+y)^2}{y}\sum_{l=1}^{\infty}\omega_l[xy(1+y)^{f-2}]^l$$

$$= \frac{y}{2} + \frac{(1+y)^2}{y}G_0(z) \qquad \text{(A.1)}$$

The radius of convergence of this infinite series is

$$z^* = (f-2)^{f-2}/(f-1)^{f-1} \qquad \text{(A.2)}$$

The explicit form of eq 2.10 is difficult to find, but we can formally express it with the help of the function $\phi^S(x,y)$:

$$\lambda\nu^{S}(x,y) = \frac{1}{n}\sum_{l,m}\frac{\omega_{l,m}}{al+bm}x^l y^m$$
$$= \frac{1}{n}\int_0^\infty \sum_{l,m} e^{-(al+bm)t}\omega_{l,m}x^l y^m \, dt$$
$$= \frac{\lambda}{n}\int_0^\infty \phi^{S}(xe^{-at},ye^{-bt}) \, dt \qquad (A.3)$$

Substitution of the explicit form (eq A.1) into this equation yields the result (eq 2.12).

Appendix B

In this Appendix we find the explicit form of z and f $G_1(z)$ as a function of ϕ. Following the ref 11, we first introduce a parameter α by the equation

$$z \equiv \alpha(1-\alpha)^{f-2} \qquad (B.1)$$

The functions $G_k(z)$ can then be explicitly written in terms of α. For example, Stockmayer[11] found

$$f\,G_0(z) = \frac{\alpha(1-f\alpha/2)}{(1-\alpha)^2} \qquad (B.2)$$

$$f\,G_1(z) = \frac{\alpha}{(1-\alpha)^2} \qquad (B.3)$$

By using the condition eq 3.4 for z, we can solve α in terms of ϕ. Substitution of the result in eqs B.1 and B.3 yields

$$z(\phi) = \frac{(1+2\xi-\eta)(f-1+\eta)^{f-2}}{(f+2\xi)^{f-1}} \qquad (B.4)$$

and

$$f\,G_1(z) = \frac{2\xi(f+2\xi)}{f-2(f-2)\xi+f\eta} \qquad (B.5)$$

where $\xi \equiv \Lambda\phi(1-\phi)/\{1+2\lambda(1-\phi)\}^2$ and $\eta \equiv \{1-2(f-2)\xi\}^{1/2}$.

References and Notes

(1) Wellinghoff, S.; Shaw, J.; Baer, E. *Macromolecules* **1979**, *12*, 932.
(2) Tan, T.; Moet, A.; Hiltner, A.; Baer, E. *Macromolecules* **1983**, *16*, 28.
(3) Boyer, R. F.; Baer, E.; Hiltner, A. *Macromolecules* **1985**, *18*, 427.
(4) Gan, J. Y.; Francois, J.; Guenet, J. M. *Macromolecules* **1986**, *19*, 173.
(5) Koltisko, B.; Keller, A.; Litt, M.; Baer, E.; Hiltner, A. *Macromolecules* **1986**, *19*, 1207.
(6) Jelich, L. M.; Nunes, S. P.; Paul, E.; Wolf, B. A. *Macromolecules* **1987**, *20*, 1943, 1948, 1952.
(7) Tanaka, F. *Macromolecules* **1989**, *22*, 1988.
(8) Tanaka, F.; Matsuyama, A. *Phys. Rev. Lett.* **1989**, *62*, 2759.
(9) Francois, J.; Gan, J. Y. S.; Guenet, J. M. *Macromolecules* **1986**, *19*, 2755. Klein, M.; Guenet, J. M. *Macromolecules* **1989**, *22*, 3716.
(10) Tanaka, F., preceding paper of this issue.
(11) Stockmayer, W. H. *J. Chem. Phys.* **1943**, *11*, 45; **1944**, *12*, 125.
(12) Flory, P. J. *Principles of Polymer Chemistry*; Cornell University Press: New York, 1953; Chapter 9.